SCIENCE CHINA
Technological Sciences

• Article •

July 2014 Vol.57 No.7: 1342–1351
doi: 10.1007/s11431-014-5587-0

Topological evolution of laminar juncture flows under different critical parameters

YOUNIS Muhammad Yamin[1*], ZHANG Hua[1], HU Bo[1] & MEHMOOD Saqib[2]

[1] *National Key Laboratory of Fluid Mechanics, School of Aeronautical Science and Engineering, Beihang University, Beijing 100191, China;*
[2] *School of Astronautics, Beihang University, Beijing 100191, China*

Received November 5, 2013; accepted May 8, 2014

Horseshoe vortex topological structure has been studied extensively in the past, traditional "saddle of separation" and new "attachment saddle point" topologies found in literature both have theoretical basis and experimental and computational evidences for support. The laminar incompressible juncture flows at low Reynolds numbers especially are observed to have new topology. Studies concerning the existence of the new topology though found in literature, the topological evolution and its dependency on various critical flow parameters require further investigation. A Particle Image Velocimetry based analysis is carried out to observe the effect of aspect ratio, δ^*/D and shape of the obstacle on laminar horseshoe vortex topology for small obstacles. Rise in aspect ratio evolves the topology from the traditional to new for all the cases observed. The circular cross section obstacles are found more apt to having the new topology compared to square cross sections. It is noted that the sweeping effect of the fluid above the vortex system in which horseshoe vortex is immersed plays a critical role in this evolution. Topological evolution is observed not only in the most upstream singular point region of horseshoe vortex system but also in the corner region. The corner vortex topology evolves from the traditional type to new one before the topological evolution of the most upstream singular point, resulting in a new topological pattern of the laminar juncture flows "separation-attachment combination". The study may help extend the understanding of the three-dimensional boundary layer separation phenomenon.

horseshoe vortex, saddle of attachment, saddle of separation, topological evolution, sweeping effect

Citation: Younis M Y, Zhang H, Hu B, et al. Topological evolution of laminar juncture flows under different critical parameters. Sci China Tech Sci, 2014, 57: 1342–1351, doi: 10.1007/s11431-014-5587-0

1 Introduction

Conventional description [1–3] of the flow separation is based on the notion of lift up of the fluid stream adjacent to the surface with the formation of the spatial vortex sheet. It may also be expressed as the lifting of the near wall vorticity into fluid space under the influence of adverse pressure gradient. Though different in description, all of the conventional theories found covenant to the concept that the vortex sheet always originates from the surface saddle. The widely used description of 3-D steady separation [2] is that the skin friction line convergent asymptote always results in the form of a spatial vortex originating from a surface saddle.

Horseshoe vortices are spawned due to the adverse pressure gradient offered by obstacles and encountered by the incoming boundary layer on its way. This vortical flow is then convected downstream by the adjacent flow along the two sides of obstacles. Conventional flow separation theory describes this spawning process of horseshoe vortices to be originating from the surface to which the boundary layer is attached, and thus is the basis of the traditional topology [4] of the laminar horseshoe vortex. The traditional topology is based on the idea

*Corresponding author (email: yamin.596@gmail.com)

that the horseshoe vortex system originates from a surface singular point with limiting stream lines leaving the surface to form a vortex sheet, thus the singular point in such a case is "saddle of separation" as shown in Figure 1 (adopted from ref. [11], Figure 1). Consistent with earlier description [4], in some of the following articles [5–7] similar description is adopted to describe the topology in their respective analysis. It is worth mentioning that the above-mentioned topological descriptions of horseshoe vortices are based on the results obtained from the qualitative flow visualization technique of smoke, dye or surface oil flow visualization.

In a theoretical analysis, Perry and Fairlie [8] observed the possible existence of a new kind of topology, where the flow instead of separating from the surface was found to be attached to the surface, by that time they couldn't present any practical example to support their analysis. They also did not negate the important implications of the interpretation of surface oil-flow visualizations. Visbal [9], in computational analysis, found the laminar horseshoe vortex structure fulfilling the new topological description (Figure 1, (adopted from ref. [11], Figure 11)) provided earlier [8]. In his results Visbal [9] found the vortex sheet to originate from a spatial saddle point and a part of the fluid from the same saddle point was attached to surface as well, making the most upstream singular point on the plate surface as "saddle of attachment". Visbal [9] further added that the convergent skin friction line asymptote was necessary but not sufficient condition for 3-D flow separation. Being entirely different in spatial description both traditional and new topologies exhibit a similar surface skin friction line pattern, also fulfill the topological rules [10].

Later a number of numerical [11–13] and experimental [14,15] studies also provided an insight into this new topology for laminar juncture flows. Hung et al. [11] using computation also observed the new topology which in their study was not only observed for the most upstream singular point but also for the corner region. They discussed the importance of the combined surface and symmetric plane analysis to describe the overall vortex topology and differentiate the "oil accumulation line", "separation line" and "attachment line", and concluded that the same surface structure may exist for different symmetry plane structures. Thompson and Kerry [12] observed the topological variation as a function of Reynolds number, and mentioned that the traditionally envisaged topology of the laminar horseshoe vortex was "incorrect". Chen and Hung [13] observed that depending on flow conditions, either the traditional or new topology may exist and that the topological rules [10] may not be fulfilled for the laminar horseshoe vortex structure when it was applied to short obstacles (when the whole upstream flow field was considered, including the leading edge of the plate).

Coon and Tobak [14], with flow visualization, observed the new topology for laminar juncture flows. They used models with different aspect ratios (*H*/*D*) yet in their investigations, they didn't observe the traditional topology in their results, and furthermore, they also encountered lack of resolution to observe the corner region. In their theoretical analysis they concluded that the three-dimensionality of the incoming flow with characteristic transverse velocity played a vital role in changing the topology of the vortex system from the traditional type to the new one.

Zhang et al. [15] further extended the idea of the new topology and provided different variants of it for the laminar horseshoe vortex system. The analysis in three different planes, namely "symmetry", "surface" and either "separation surface" or "attachment surface" planes for the traditional or new topology respectively was provided in detail, along with discussion about the difference in the "conventional attachment" and "attachment saddle point". Previously Wang et al. [16] using numerical simulations presented that two different space structures (traditional and new) exhibited similar skin friction line pattern, which later was also found by Zhang et al. [15] shown in Figure 1. In the current study only symmetry plane structures are observed, it is extremely difficult to observe the surface structure using PIV due to experimental limitations. In another article Zhang et al. [17] presented the relationship between the Lighthill's three-dimensional separation [2] mode (traditional) and the attachment saddle point (new) structure. They observed that the Lighthill's separation model was valid not only for the traditional topology but was equally effective for the new one. A noticeable fact is that the new topology is found to be the outcome of either qualitative flow visualization analysis or computational work. Studies though provided

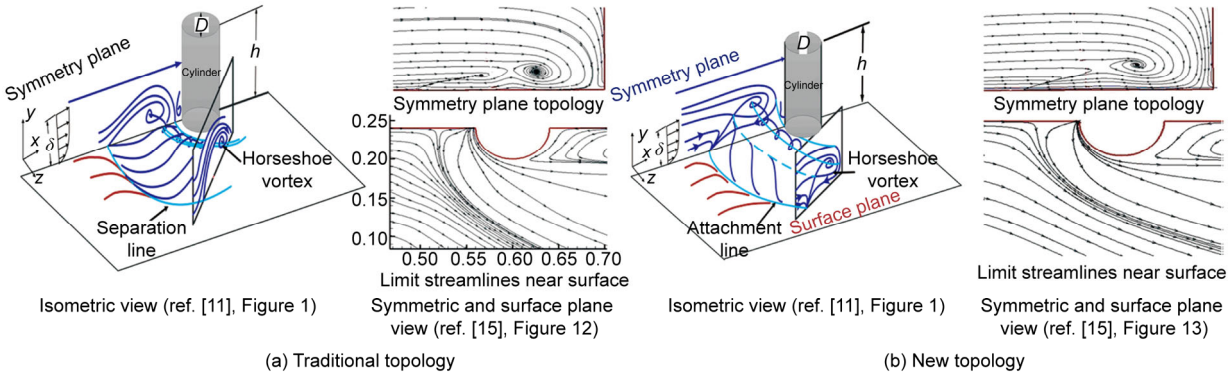

Figure 1 (Color online) Comparison of conventional and new horseshoe vortex topologies.

the evidences about the existence of both the traditional and new topologies, yet just a few parametric studies are carried out and a little are known about evolution of topology of the laminar horseshoe vortex system. A number of flow parameters including obstacle width based Reynolds number (Re_D), boundary layer thickness (δ), aspect ratio (H/D), cross-sectional shape of the obstacle etc. may cause the vortex system to change from one topological form to other. In the present study the horseshoe vortex topology for short cylinders with square and circular cross sections will be observed using PIV.

The effect of aspect ratio (H/D), boundary layer thickness parameter (δ^*/D), and obstacle shape on the topology of the horseshoe vortex will be examined at a fixed Reynolds number Re_D=600 for short cylinders. In the last part, the relation between the most upstream singular point and corner region singular point is observed and evaluated with the singular point analysis [10], which has also been used in the past [4,6,9,11,13–15] for similar topological analysis of laminar juncture flows. This study will be helpful to further extending the understanding of the concept of "saddle of attachment" in juncture flows.

2 Experiment platform and procedure

The experiments were conducted in the water channel of the Institute of Fluid Mechanics of Beihang University. The test section of the water channel was 400 mm×400 mm in cross section with length of 2 m and achievable free stream velocity ranged from 1 to 10 cm/s. The experiments were carried out using a 2-D PIV system which consisted of dual-cavity pulse Nd:Yag laser with Δt=200–600 ns and power of 200 mJ/pulse, laser sheet arm, laser pulse synchronizer and CCD camera with spatial resolution of 2448 pixels× 2050 pixels with data sampling frequency of 30 frames/s. A MACRO 105 mm F2.8 EX DG lens was attached to get a better and detailed view of the flow structure. The particles seeded in the water for flow visualization were Aluminum-di-Oxide Al_2O_3 particles with diameter of 400 nm and the specific gravity was about 3.4–4.0. The frame-to-frame cross correlation technique was applied to calculate the velocity vectors in this study, using "Micro Vec. V3.3.1" (developed by the World Technology Development Co., Ltd. Beijing) which integrates the PIV, PTV, concentration and particle size analysis and field analysis module.

Small obstacles of square and circular cross sections with aspect ratio ($0.66 \leqslant A.R. \leqslant 3.33$) were experimented in this study, with ratio of diameter of the cylinder to boundary layer thickness $D/\delta \leqslant 3$. Reynolds number based on free stream velocity ($\boldsymbol{U}_\infty$) and obstacle's width/diameter (Re_D =600) was kept fixed. Models were placed on different locations so as to get different boundary layer parameters (δ^*/D). Before placing the model at any particular position, boundary layer thickness was measured at each position, where later the leading edge of the model lay to make sure that the δ^*/D was kept fixed. A comparison between the results of the experimental boundary layer and those of the Blasius boundary layer was made as shown in Figure 2 at three positions. The difference between the heights of the boundary layer observed in experiments (δ_{Exp}) and those of Blasius (δ_B) at various stations remained ±5% ($\delta_{\text{Exp}}=\delta_B \pm 0.05\delta_B$) for all the cases.

3 Results and discussion

The horseshoe vortex system as mentioned earlier is studied for a number of interesting fluid mechanics phenomena, one of which is the new topology [9] where the vortex sheet originates from a spatial saddle point, instead of a surface saddle point [4] in accordance with classical flow separation theories. A number of studies though observed the saddle of attachment as the dominant flow topology at low Reynold numbers, for the incompressible flow situations (a focus of this study), a careful visualization study is required to clearly observe which topology is dominant and under what conditions it exists.

The horseshoe vortex structure for various δ^*/D was investigated, where for all the cases experimented in the current study for both the square and circular cylinders the horseshoe vortex system was found to be stationary, no oscillations in either primary or secondary vortices were observed. Chang et al. [18] observed that the three parameters, aspect ratio (H/D), Reynolds number (Re_D) and H/δ influenced the steady horseshoe vortex structure significantly. In the present case the results indicate that the overall structure for the circular cylinder consists of two clear primary vortices with no visible secondary vortex between the two at δ^*/D=0.115 and H/D=0.67. The vortex system reduces from

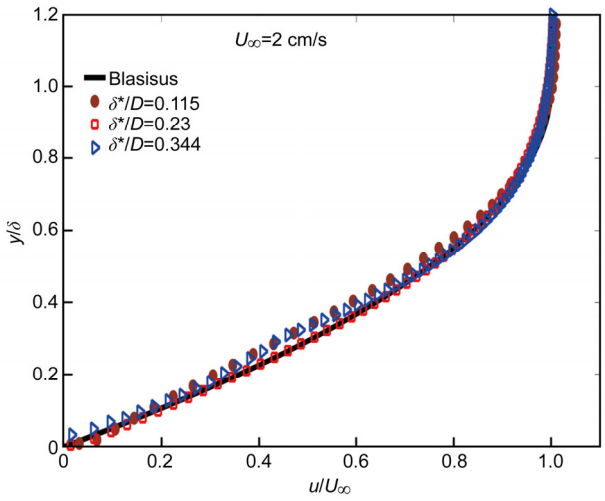

Figure 2 (Color online) Boundary layer, three different cases compared with Blasius.

"two" to "single" primary vortex, horseshoe vortex system with increasing δ^*/D, though the size of the separated region increases, yet the number of vortices decreases. Similarly, increasing the aspect ratio also causes the vortex system to reduce from "two" to "single" primary vortex, horseshoe vortex system, the separated region though has increased, the number of vortices decreases. On the other hand for the square cylinder, the horseshoe vortex system is a three−vortex system (two primary and one secondary vortices) for δ^*/D=0.115 and H/D=0.67. With the increase in aspect ratio, individual vortices in the vortex system reduce in size, or overall vortex system may also reduce in number of vortices that the vortex system comprises.

The variation of the location of the primary vortex core for the increasing aspect ratio (H/D) and δ^*/D upstream of the leading edge of the obstacle is shown in Figure 3. Results reveal that the non-dimensionalized distance of the primary vortex core (X_P/D) upstream on the leading edge of the obstacle changes with both of the above-mentioned parameters. The results show that the variation in (X_P/D) is not significant for both circular and square obstacles at low δ^*/D, but increases significantly for higher δ^*/D values, for increasing H/D. On the other hand at the fixed H/D, change in δ^*/D also varies the vortex core location significantly, distance (X_P/D) increases with the increase in δ^*/D. The variation in X_P/D is observed relatively small at low aspect ratios for different δ^*/D, which gradually increases with increasing aspect ratios for both cross-section obstacles investigated. The obstacle cross sectional shape also plays a role in this variation, the distance (X_P/D) is found small for circular cross sections compared to square ones. The variation in (X_P/D) is also higher for the square obstacle than for circular, for increasing either δ^*/D or H/D.

In line with the changes horseshoe vortex experiences in overall structure, topology changes as well. Considering the case of δ^*/D=0.115 (Figure 4), for circular cylinder, increasing *A.R.* (H/D) causes the vortex system to change from the two (P_1, P_2 at H/D=0.66) to a single (P_1 at H/D=2.33) primary vortex, horseshoe vortex system. The change in the overall vortex structure is clear from both the streak and stream lines for two aspect ratios, this change is not only limited to the overall vortex structure, but also results in the topological evolution (from traditional type to the new one). Let us have a detailed analysis to show how the topology of the overall vortex system evolves. The near wall region adjacent to the most upstream singular point for four different aspect ratio models is shown at the left half of Figure 4, the primary vortex labeled as P_1 does not change qualitatively so it is ignored in this discussion. The region of the streak lines for H/D=0.66 and 2.33 enclosed in the white dashed line box on the right hand side of Figure4 is shown on the left side with the addition of the same region of H/D=1.33 and 1.66 case. For H/D=0.66 it is clear from both streak and streamlines that the vortex system is composed of two primary vortices with a half saddle of separation Ss', as the originating point of the vortex sheet. The vortex sheet then roles up to form the second primary vortex labeled P_2 shown on the right of Figure 4 and labeled as node N on the left close-up view of the same figure. This confirms the existence of the traditional topology of the horseshoe vortex system at closely similar experimental conditions to that of Coon and Tobak [14] who failed to observe any such result.

At aspect ratio H/D=1 (not shown in Figure 4) the topology is still observed to be traditional, but at H/D=1.33 the near wall vortex pattern adjacent to the most upstream singular point is not clear. The streamlines coming from upstream and reversed flow moving upstream are found to cross each other. This can be a special result of symmetrically three-dimensional laminar separation (η_x/ξ_y=1) [8], when the spatial plane singular point near the surface changes from separation (saddle) type to attachment (node) type or vice versa. For H/D=1.66 the vortex structure now is found to have an additional space saddle S which diverts some incoming fluid to vortex P_2 (N) and some to the surface singular point NA' (half node of attachment) which now is the most upstream singular point. During this process of topological shift (from traditional to new) at H/D=1.33, the nature of the most upstream near wall, singular point is not clear, on the other hand for lower and higher aspect ratio cases, the two different topological patterns are clearly observed,

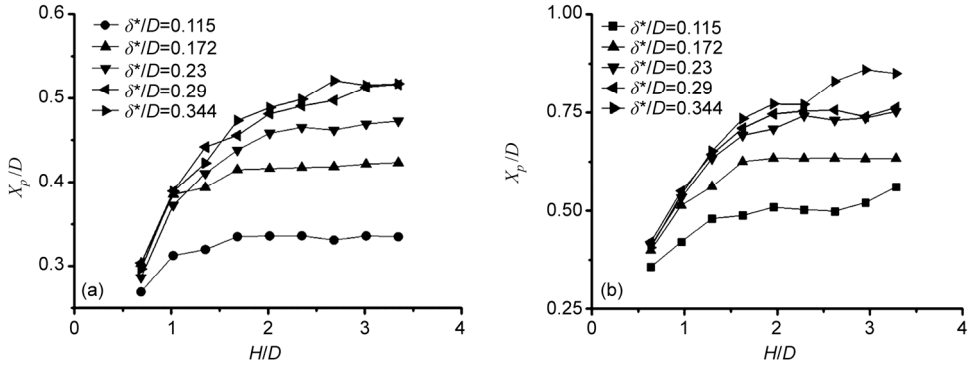

Figure 3 Variation of primary vortex core location upstream in juncture leading edge. (a) Circular cylinder; (b) square cylinder.

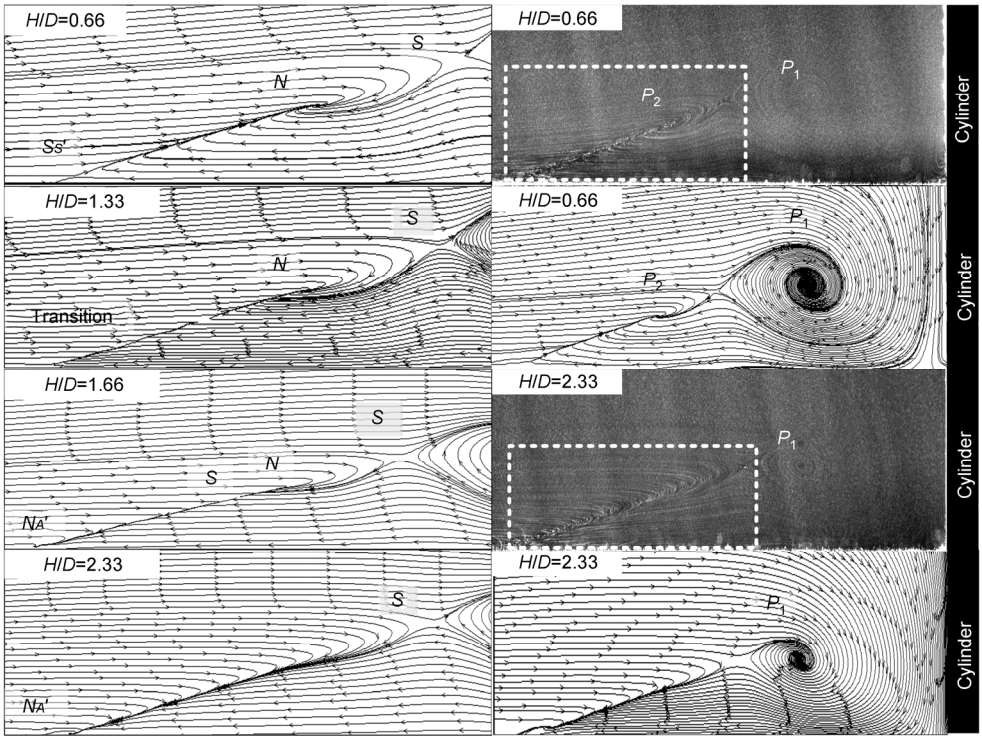

Figure 4 Effect of aspect ratio (H/D) on horseshoe vortex topology circular cylinder $\delta*/D$=0.115.

making it adequate to calling topology at H/D=1.33 as transitional topology.

For further high aspect ratio the 2nd primary vortex completely disappears gradually with a saddle nodal pairwise annihilation (fold bifurcation) [19]. Only one primary vortex P_1 is left (for H/D>1.66 (Figure 4)) which starts from a spatial saddle S, a part of the fluid from this saddle goes to this primary vortex and the other half is deflected towards the surface converting the most upstream singular point is a half node of attachment N_A' in the symmetry plane.

The shape of the cylinder is found to have important influence, not only on the overall vortex system, but more importantly on the topological behavior. At similar flow conditions the circular cylinder may have less number of vortices compared to the square cross section. Figure 5 shows the topological change in the horseshoe vortex system with the varying aspect ratios for both the circular and the square cylinders. This clearly indicates a prior evolution of topology for the circular cylinder compared to that of the square cylinder, concluding that the circular cylinder is more apt to the attachment topology than separation with the rise in aspect ratio and $\delta*/D$. In order to observe the topological evolution of laminar juncture flow, the incoming boundary layer for the circular cylinder case is divided into three parts, A, B and C (at the point of the most upstream singular point) (Figure 6) such that the whole horseshoe vortex system is composed of the fluid within this height (A+B+C). "A" is the downstream moving fluid within the solid surface (plate) and the first spatial saddle (S), "B" is the amount of fluid which makes up the primary vortex closest to the cylinder (labeled as P_1 in Figure 4) and "C" is the fluid which moves upstream (after reversal), and interacts with the incoming flow A (between most upstream spatial saddle S and most upstream surface singular point). The contribution of the boundary layer fluid to A, B and C for different δ^*/D with the varying aspect ratios is shown in Figure 6, horseshoe vortex system in front of the circular cylinder is considered. Under all these conditions, no visible secondary vortex is observed, so the vortex system in Figure 6 is drawn without the secondary vortex. In each case with the rise in the aspect ratio, a slight increase in height, "A" is observed, on the other hand, B reduces significantly, and C increases substantially. The variation in the heights A, B and C follows a similar pattern for all δ^*/D cases, but the total amount of the boundary layer fluid contributing to the vortex system reduces with $\delta*/D$ shown in Figure 6.

Rodríguez et al. [20] observed the important influence of the flow velocity gradients of the fluid above the horseshoe vortex in which the horseshoe vortex was immersed. According to their observations, at the low aspect ratio the vortex system is swept strongly by this fluid due to higher velocity gradients of the fluid above the horseshoe vortex system. Contrary to this, at the high aspect ratio due to the influence of the blockage of the obstacle, the velocity gradient reduces conversely, the sweeping effect as well. On the other hand at the higher aspect ratio the quantity of the fluid entrained by the horseshoe vortex increases (in accordance with previous results [20]). At the small aspect

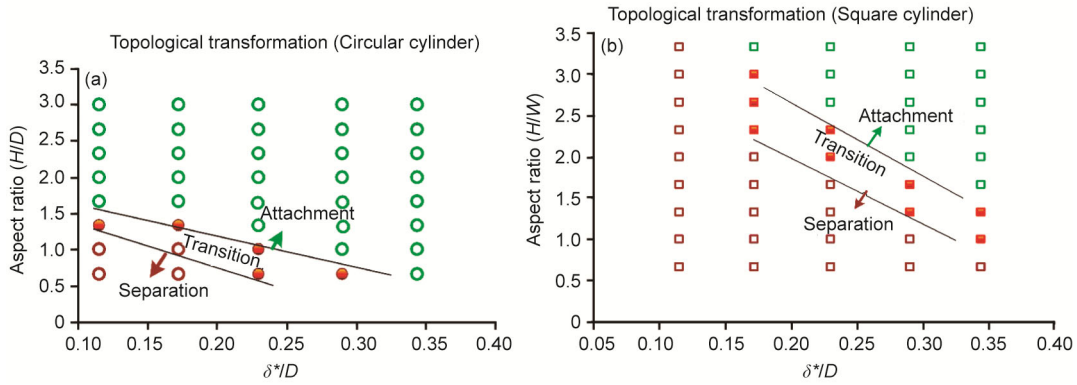

Figure 5 (Color online) Impact of aspect ratio on horseshoe vortex topological evolution. (a) Circular cylinder; (b) square cylinder.

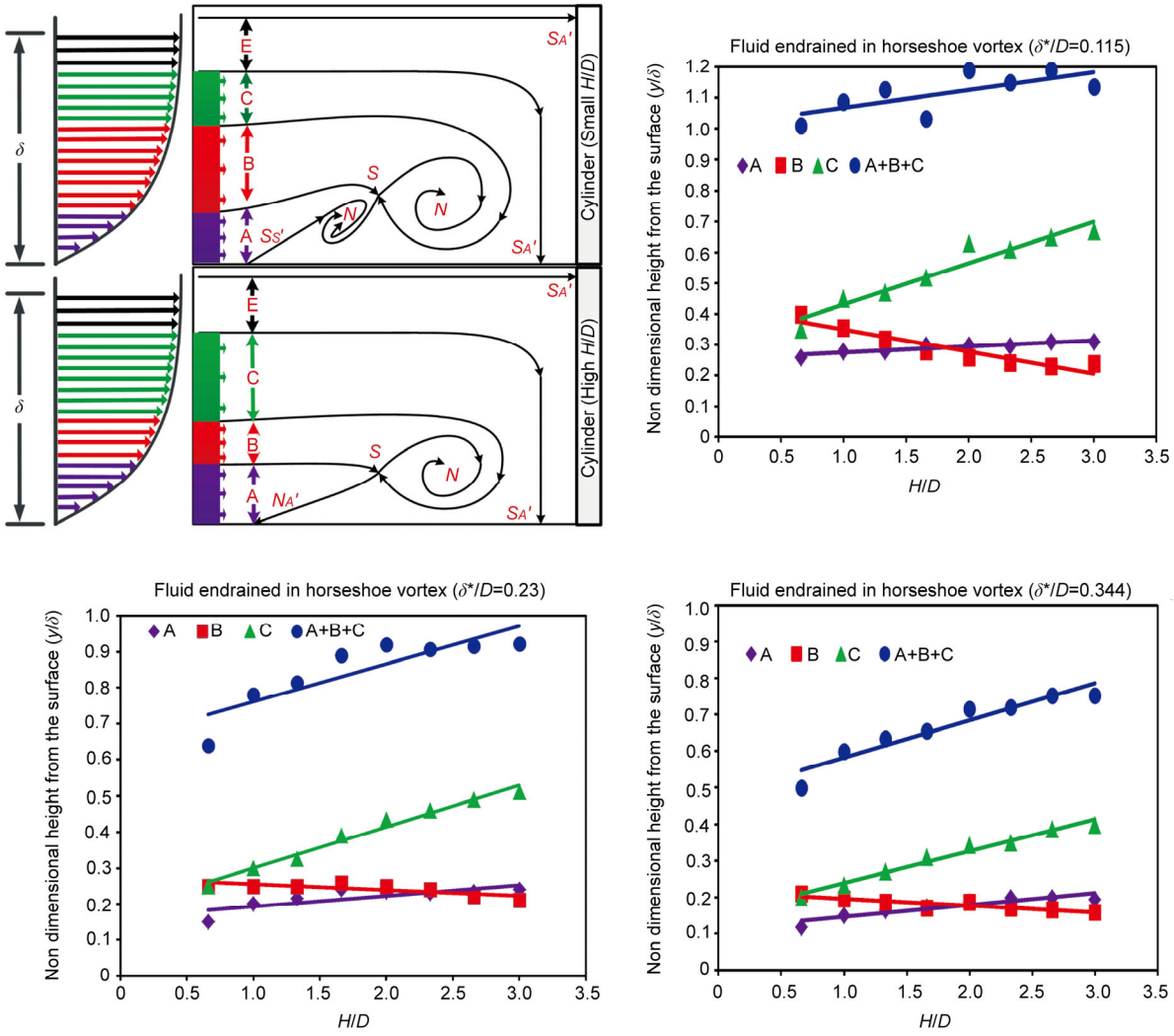

Figure 6 (Color online) Variation of boundary layer fluid entrained by various sections of horseshoe vortex for circular cylinder at different δ^*/D.

ratio the less quantity of fluid entrained by the vortex system undergoes a strong sweeping affect this increases the amount of the primary vorticity of the vortex system. An upward pull experienced by the limiting streamlines near the most upstream singular point due to this strong sweeping effect causes the fluid stream to lift from the surface and vortex system undergoes traditional separation (Figure 4, H/D=0.66).

At the higher aspect ratio the fluid quantity entrained by the vortex system increases, on the other hand, sweeping effect reduces considerably due to the blockage of the obstacle. The outcome of these factors results in the reduction

of fluid quantity B and increase in C (shown in Figure 6), and this reduction in B is due to the reduction of the sweeping effect. The quantity C now at one end increases the size of the vortex system by taking the upstream singular point on the plate surface further upstream, while on the other end, it enables more quantity of the fluid to interact with the upcoming fluid "A". Under these flow conditions the horseshoe vortex system at higher aspect ratio reduces from "two vortices" to a "single vortex" structure, evolving the most upstream singular point from the traditional topology to new one (Figure 4 *H*/*D*=2.33). Visbal [9] and Coon and Tobak [14] did not consider the important influence of sweep of the fluid above the vortex system on topological evolution. Though Visbal [9] used the model with *H*/*D*=2 in his numerical analysis, he used a case of cylinders confined between two walls, thus the sweeping effect is small in such case and the associated topology is of the new type. The stronger sweeping effect associated with the strong free end effect of the square cylinder compared to that of the circular cylinder delays topological evolution to higher aspect ratios at similar flow condition (Figure 5).

Analyzing the vortex system with the counter rotating secondary vortex, a case of the square cylinder is considered, as shown in Figure 7, all the results are taken with similar

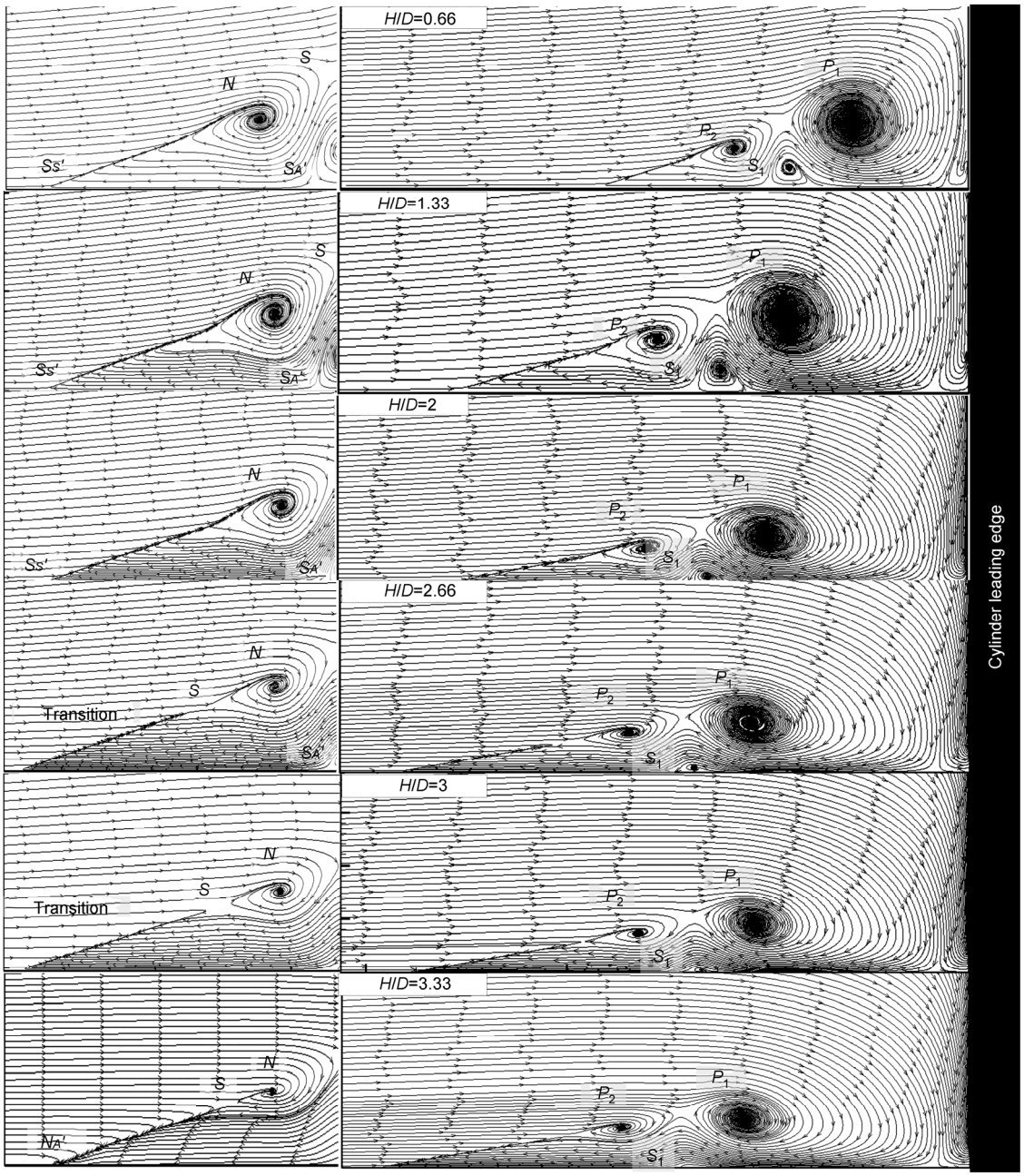

Figure 7 Topological evolution and secondary vortex (δ^*/D=0.172).

spatial coordinates in order to make them readily comparable. With the change in aspect ratio, the size of the secondary vortex S_1 increases to a certain level (Figure 7, H/D=1) and then reduces considerably (Figure 7). The increase in C (discussed earlier) accompanied by a reduction in size (fluid entrained) of the secondary vortex (S_1) makes more and more reversed flow (in turn, secondary vorticity) to interact with A, and contributes to topological evolution. A clearly visible vortex S_1 (Figure 7, H/D=0.66) during the topological evolution also diminishes and results in a very small secondary vortex (hardly visible, Figure 7, H/D=3.33). The streamlines in Figure 7 at H/D=2.66 and 3, behave similar to what is already observed in Figure 4 for H/D=1.33. The streamlines seem to cross, it is a special case of 3-dimensional laminar flow separation and is already explained in Section 3.2. Under this dispersion of the secondary vorticity towards the most upstream singular point the small amount of incoming vorticity content of the incoming flow (A) experiences a downward pull and thus shifts topology from traditional type to new one.

The traditional topology [4] of the juncture flows consists of a small corner vortex near the plate/obstacle juncture. In this case not only the most upstream singular point, but also the corner vortex initiates from a "half saddle of separation", the former originates from the plate surface, whereas the latter from the cylinder surface. Visbal [9] in his computed results of the steady laminar horseshoe vortex system did not get a clear corner vortex, still he insisted on sketching a corner vortex (originating from a half saddle of separation from the cylinder surface) in his topological description. Chen and Hung [13] later found that not only the most upstream singular point in laminar juncture flows was a "saddle of attachment" but also the corner vortex. He thus presented a topological pattern which is different from those of the earlier ones. Coon and Tobak [14] in their flow visualization were unable to present any results near the corner region, due to the resolution problem of their equipment. In the current study, a focused and careful experimentation is carried out to find out which topological picture of the above three [4,9,13] really exists, and how it varies with change in aspect ratio for laminar juncture flows. Other than just observing the topology of the corner vortex, a relation of topological evolution of the most upstream singular point to that of the corner region topological transformation is also investigated.

Different topological patterns are observed with varying aspect ratios repeatedly and it has been found that not only the most upstream singular point topology evolves from traditional to new, but also the corner region topology undergoes this evolution process. The difference among the two is that the former is concerned with the flow along the plate and the later on the flow along the cylinder. At low aspect ratios the most upstream singular point on plate surface is a half separation saddle point (Ss′) (symmetric axis), on the other hand, the corner region also exhibits a clear vortex which originates from a half separation saddle point (Ss′) on the cylinder surface (Figure 8, H/D=0.66). The reason for such structure is again the "sweeping" of the horseshoe vortex system by the fluid above it, making the fluid to accelerate at higher rates. A stronger interaction of the primary vortex (closest to the cylinder) with that of the cylinder surface results in a separation topology in the corner region, with the formation of a counter clockwise rotating vortex. This combination of topologies of the most upstream singular point and the corner region is named here "separation-separation combination" or traditional topology [4]. Increasing the aspect ratio changes the corner region topology (Figure 8, H/D=1.33), and now the half saddle of separation *Ss′* on the cylinder surface has changed to half node of attachment *NA′*, though the most upstream singular point is still *Ss′*. The primary vortex closest to the cylinder in this case (H/D=1.33) has already moved quite a distance upstream from the cylinder leading edge, also due to a significant reduction in the sweep (due to the blockage of the obstacles having high aspect ratio), the interaction of the primary vortex with that of cylinder surface is significantly weak. Being pointed out by Coon and Tobak [14] the three-dimensionality plays its role at higher aspect ratio, the corner region transforms topology to the new type under all such conditions. This combination of the topologies of two regions is called "separation-attachment combination" where the most upstream singular point has not transformed topology but the corner region topology has changed to attachment type, such structure has not been observed in the previous text to the authors' knowledge. Here this topological combination is considered as a variant form of traditional topology, because the most upstream singular point still is half saddle of separation *Ss′* (traditional topology). With the further increase in aspect ratio (Figure 8, H/D=2 and 3), the most upstream singular point also evolves to half node of attachment *NA′*, establishing an "attachment-attachment combination" or new topology [13]. The investigation not only reveals the topological structure (Figure 9) of the laminar horseshoe vortex observed by Baker [4] (Separation-Separation Combination, traditional topology), and by Chen and Hung [13] (Attachment -Attachment Combination, new topology), but also a new topological pattern is observed. The new topological structure "separation-attachment combination" is different from the former in the corner region and different from the latter in the most upstream singular point topology. On the other hand, current flow visualization results support the attachment saddle point topology (new topology) proposed by Chen and Hung [13], rather than that of Visbal [9], in the corner region. All the experiments carried out in this study exhibit that the corner region always transforms topology (from traditional to new) prior to the topological evolution of the most upstream singular point, with increase in aspect ratio. Based on the results it is proposed that the attachment saddle point topology (new topology) of the horseshoe vortex will

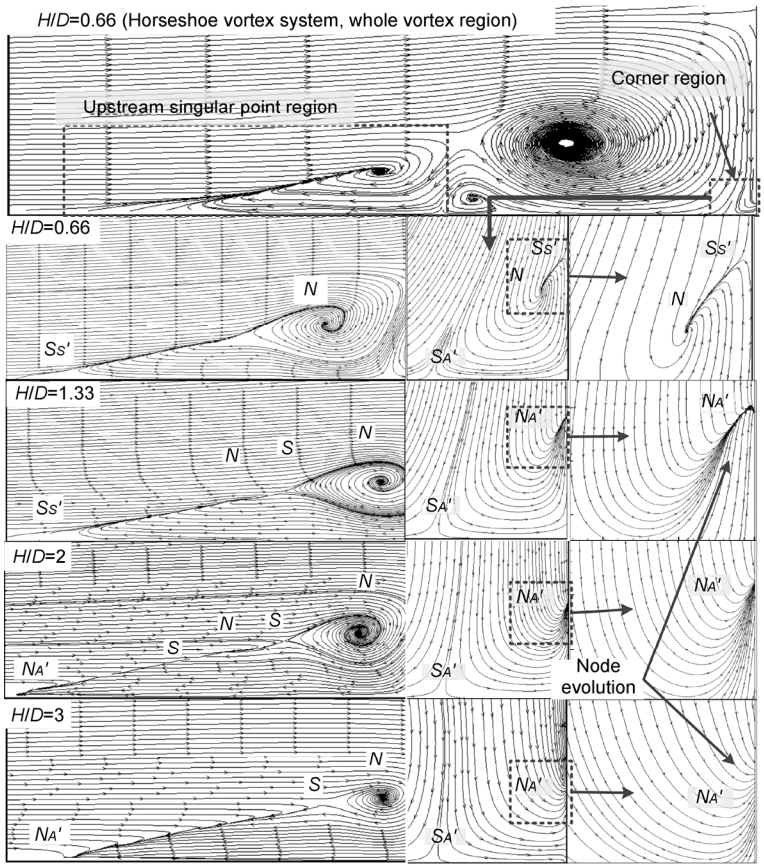

Figure 8 Relation between the most upstream singular point region and corner region.

always have half node of attachment N_A' on the cylinder surface in the corner region, which is in accordance with Chen and Hung [13]. Traditional topology [4] may either have a half saddle of separation S_S', or a half node of attachment N_A' (Separation-Attachment Combination) in the corner region, contrary to this, new topology at no point is observed to have a corner vortex (originating with the separation saddle point S_S' on the cylinder surface) as is described by Visbal [9]. An important observation is that after the topological shift, the node of attachment also reduces its strength gradually from being a "focused" (Figure 8, H/D=1.33 and 2) to a "distracted" (Figure 8, H/D=3) one with the increase in aspect ratio. A "node evolution" (Figure 8) in the corner region further exhibits the weaker interaction of the primary vortex with that of the cylinder surface even after topological evolution.

The singular point topological rules presented by Hunt et al. [10] have been widely used for topological analysis of laminar juncture flows [4,6,9,11,13–15] in symmetry plane. The singular point index of the local symmetry plane must fulfill the following criterion:

$$\left(\sum N+\frac{1}{2}\sum N'\right)-\left(\sum S+\frac{1}{2}\sum S'\right)=0. \qquad (1)$$

Here N and N' represent the node index and half node index respectively, and S and S' represent the saddle point index and half saddle point index, respectively. We all know that the above rule is valid for separation-separation combination [4] (traditional topology), and for attachment-attachment combination [13] (new topology) it is equally applicable to "separation-attachment combination" as well. With N=3, S=1, S_S'=2, S_A'=3, N_A'=1, the above relation is satisfied and provided topological existence of such "separation-attachment combination" of the horseshoe vortex system as well.

4 Conclusion

The horseshoe vortex system for small cylinders is studied at Reynolds number Re_D=600 for the square and circular cross sectional cylinders, and varying aspect ratios (H/D). With the increasing aspect ratio H/D for all the cases investigated, the topological structure is found to evolve from traditional, separation type to new, attachment type. The most upstream singular point changes from "saddle of separation" to "saddle of attachment", with variation in fluid quantity entrained by different portions of the horseshoe vortex system. Increase in δ^*/D for all the cases shows that the saddle of attachment topology is more likely to occur

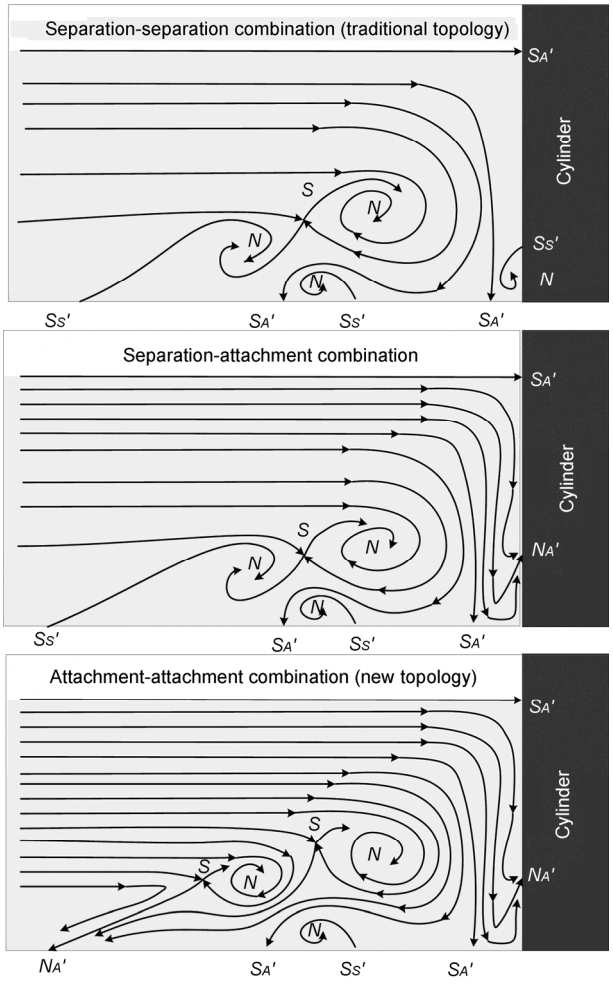

Figure 9 Comparison of the three different types of laminar horseshoe vortex topologies observed in the current study.

with rising δ^*/D.

"Sweeping" effect due to the velocity gradients of the fluid above the horseshoe vortex system plays a very important role in topological evolution, for strong sweeping effect, the topology predominantly is of traditional type, for weaker, it evolves to new type. Circular cross section cylinders are more apt to having new topology than the square at relatively low aspect ratios due to the small free end contribution in sweep.

A variant form of the traditional vortex topology is observed where the corner region is found to have a half node of attachment on the cylinder surface, and fulfills the topological rules. Earlier topological evolution in the corner region rather than the topological evolution of the most upstream singular point results in that new topology should have a half node of attachment on the cylinder surface rather than half saddle of separation (with the corner vortex) in the corner region.

This work was supported by the National Natural Science Foundation of China (Grant No. 11372027).

1 Maskell E C. Flow Separation in Three Dimensions. Farnborough: Royal Aircraft Establishment, 1955
2 Lighthill M J. Laminar boundary layers. In: Rosenhead L, ed. Introduction Boundary Layer Theory, chap. 2. Oxford: Oxford University Press, 1963
3 Wang K C. Separation of Three-Dimensional Flow. NASA STI/Recon Technical Report N, 1976
4 Baker C J. The laminar horseshoe vortex. J Fluid Mech, 1979, 95: 347–367
5 Khan M J, Ahmed A, Trosper J R. Dynamics of the juncture vortex. AIAA J, 1995, 33: 1273–78
6 Khan M J, Ahmed A. Topological model of flow regimes in the plane of symmetry of a surface-mounted obstacle. Phys Fluids, 2005, 17: 1–8
7 Wei Q D, Chen G, Du X D. An experimental study on the structure of juncture flows. J Vis, 2001, 3: 341–348
8 Perry A E, Fairlie B W. Critical points in flow patterns. Adv Geophys, 1974, 18: 299–315
9 Visbal M R. Structure of laminar juncture flows. AIAA J, 1991, 29: 1273–1282
10 Hunt J C, Abell C J, Peterka J A, et al. Kinematical studies of the flows around free and surface-mounted obstacles: Applying topology to flow visualization. J Fluid Mech, 1978, 86: 179–200
11 Hung C M, Sung C H, Chen C L. Computation of saddle point of attachment. AIAA J, 1992, 30: 1561–1569
12 Thompson M C, Kerry H. Prediction of vortex junction flow upstream of a surface mounted obstacle. In: 11th Australasian Fluid Mechanics Conference. University of Tasmania, Hobart, Australia, 1992
13 Chen C L, Hung C M. Numerical study of juncture flows. AIAA J, 1992, 30: 1800–1807
14 Coon M D, Tobak M. Experimental study of saddle point of attachment in laminar juncture flow. AIAA J, 1995, 33: 88–92
15 Zhang H, Younis M Y, Hu B, et al. Investigation of attachment saddle point structure of 3-D separation in laminar juncture flow using PIV. J Vis, 2012, 15: 241–252
16 Wang X, Zhang H, Wang H, et al. New 3-D separation structure in juncture flows (in Chinese). J BUAA, 2010, 36: 1461–1464, 1479
17 Zhang H, Hu B, Younis M Y, et al. Attachment saddle point topology and evolution of 3-D separation in juncture flow (in Chinese). J BUAA, 2012, 38: 857–861
18 Lin C, Ho T C, Dey S. Characteristics of steady horseshoe vortex system near junction of square cylinder and base plate. J Engg Mech, 2008, 134: 184–197
19 Tricoche X, Wischgoll T, Scheuermann G, et al. Visualizatio of very large data sets, topology tracking for the visualization of time-dependent two dimensional flows. Comput Graph, 2002, 26: 249–257.
20 Rodríguez Y D M, Romero M R, Ramos P M, et al. The laminar horseshoe vortices upstream of a short cylinder confined in a channel formed by a pair of parallel plates. J Vis, 2006, 9: 309–318